

Numerical Analysis of Magnetic Nanoparticles Penetration within the Cancerous Tumor Tissue under Influence of External Magnet

Sayyed Mohammad Ali Ne'mati, Majid Ghassemi* and Azadeh Shahidian

Mechanical Engineering, K. N. Toosi University of Technology, Tehran, Iran

Abstract: Using the great magnetic drug carriers (MDCs) is proposed mechanism to reduce and increase the toxic drugs penetration within the healthy and cancerous tissues, respectively. The purpose of current study is to investigate the penetration of magnetic drug carriers within the cancerous tumor tissue under the influence of external magnet. In order to solve the coupled governing equations an in house finite volume based code is developed and utilized. Capillary wall and tumor tissue is modelled as a saturated porous media. Results show the penetration of MDCs into the tumor in the absence of magnetic field is minimal and is limited to the surface of the tumor. On the other hand, under the influence of external magnet the penetration of MDCs within the tumor increases exponentially.

Keywords: Cancer, tumor, drug delivery, magnet, nanoparticle.

1. INTRODUCTION

Chemotherapy as one of the most utilized cancerous tumor treatment methods could introduce undesired side effects in the healthy organs [1]. The chemotherapy side effects can be reduced by reducing the level of drug concentration in healthy tissues. In order to minimize the drug concentration in healthy tissues, using the large drug carriers is an attractive method because they do not penetrate the healthy tissues (except liver, spleen and bone marrow) where pores of capillaries wall are smaller than 60nm [2, 3].

However, the large carriers do not penetrate deeply into the cancerous solid tumors [4]. This is due to the low filtration rate and also outward flow of interstitial fluid which limits the drug delivery only to diffusion from the tumor surfaces [5]. Also, the carrier size has direct effect on the drug diffusion.

In order to improve the penetration issue, magnetic drug carriers (MDCs) are used. For drug delivery, magnetic nanoparticles are loaded with drugs, coated with biocompatible coatings and are injected into the human vessel. The loaded particles move through the vessel and are aggregated where the magnetic field is applied.

Drug delivery by magnetic drug carriers (MDC) has been the topic of many researches in the medical field. The issue of drug delivery inside a blood vessel has studied. For instance Shaw and Murthy [6], Khashan and Furlani [7], Sharma *et al.* [8] and Grief and Richardson [9], ignored the effect of MDCs on the

velocity field. Also, Habibi and Ghassemi [10], Li *et al.* [11], Cao *et al.* [12] and Habibi *et al.* [13] investigated the blood flow and MDCs concentration in 2D channel without ignoring the effect of MDCs on the velocity field. But these investigations limited to blood vessel and did not study the MDCs distribution within the tissue. In addition, Nacev *et al.* [14] numerically investigated the behaviour of MDCs distribution in and around the blood vessel under influence of external magnet by some simplifications such as Ignoring the horizontal magnetic force and effect of MDCs on blood flow and considering no coating for nanoparticles. Also, the MDCs diffusion coefficient in the vessel wall and tissue are not calculated. They find that there are three prototypical behaviours (blood velocity dominated, magnetic force dominated, and boundary layer formation). Also some fine studies such as Klinbun *et al.* [15], Khanafer *et al.* [16] and Keangin *et al.* [17] investigated the effect of electromagnetic field on the transport through biological and porous media. But there is no nanoparticle in these works.

As mentioned, to date there is no good investigation which calculates the penetration of MDCs within the cancerous tumor tissue under the influence of external magnet.

The purpose of current study is to deliver the magnetic drug carrier (MDC) to the cancerous tumor tissue, enhance the penetration of drug and increase the effectiveness of the treatment. In this study, the numerical investigation of MDCs penetration into the cancerous tumor under the influence of non-uniform magnetic field is presented. Also the physical parameters that affect the MDCs distribution are studied. The MDCs diffusion coefficients in the capillary as well as its wall and the tumor tissue are considered as variable and calculated. These coefficients are

*Address correspondence to these authors at the Vanak Square, Molla-Sadra Ave., Pardis Ave; P. O. Box 19395-1999; Tel: (+98 21)84063244; Fax: (+98 21)88644748; E-mail: Ghasemi@kntu.ac.ir

functions of MDCs diameter, pore size of capillary wall, tissue porosity and etc.

2. PROPOSED MODEL

The MDCs penetration from a peripheral capillary to tumor tissue under the influence of external magnet is modelled. Figure 1 shows the schematic model of the capillary, its wall (the Endothelium layer), the tumor tissue and external magnet. As shown, the capillary assumed as 2-D channel. Also the Endothelium layer and the cancerous tissue is saturated porous media. The channel width (w) and length (l) are as 40 microns and 6mm, respectively and Endothelium layer thickness is 0.5 microns [18, 19, 20]. The tumor tissue has 4mm thick. The external magnet is cylindrical with 4mm diameter and is placed on the top of the tumor tissue.

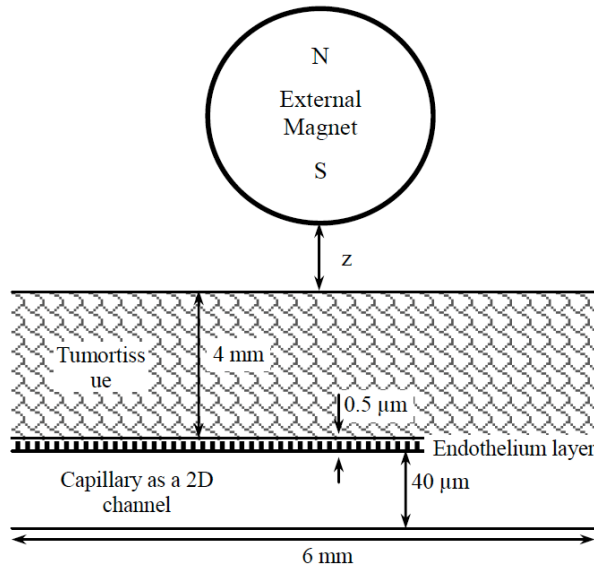


Figure 1: Schematic model of capillary, its wall and tumor tissue.

The blood is treated as Newtonian and its viscosity and its density are 3.45cP and 1050kg/m³, respectively.

The MDCs structure is depicted in Figure 2. As shown the MDCs are core-shell shape (spherical core with 5nm biocompatible shell). The core is mixture of super paramagnetic nanoparticles in polymer sphere. The volume of MDC (∇_{MDC}) is sum of core sphere volume and coating volume. Total volume of magnetic nanoparticles (∇_{MNP}) is 0.7 of core sphere volume. Therefore total MNP's volume (∇_{MNP}) of single MDC is as follow:

$$\nabla_{MNP} = 0.7(\nabla_{MDC} - \nabla_{Shell}) \quad (1)$$

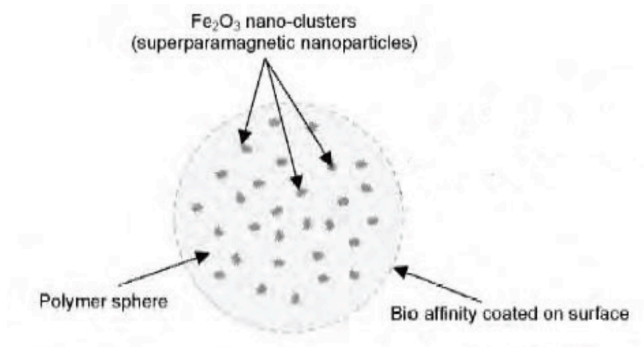


Figure 2: MDCs structure.

3. GOVERNING EQUATIONS

The governing equations for capillary, Endothelium layer and tumor tissue explained in the following section separately.

3.1. Inside the Capillary

In this study blood is incompressible and the mass and momentum equations are as follow, respectively [21]:

Continuity equation:

$$\frac{\partial u}{\partial x} + \frac{\partial v}{\partial y} = 0 \quad (2)$$

Horizontal momentum equation:

$$\rho \frac{\partial u}{\partial t} + \rho \left(u \frac{\partial u}{\partial x} + v \frac{\partial u}{\partial y} \right) = -\frac{\partial p}{\partial x} + \mu \left(\frac{\partial^2 u}{\partial x^2} + \frac{\partial^2 u}{\partial y^2} \right) + F_x \quad (3)$$

Vertical momentum equation:

$$\rho \frac{\partial v}{\partial t} + \rho \left(u \frac{\partial v}{\partial x} + v \frac{\partial v}{\partial y} \right) = -\frac{\partial p}{\partial y} + \mu \left(\frac{\partial^2 v}{\partial x^2} + \frac{\partial^2 v}{\partial y^2} \right) + F_y \quad (4)$$

Where F_x is the horizontal and F_y is the vertical component of magnetic body force, which applied to blood.

The magnetic body force is given by:

$$\vec{F} = \vec{F}_1 n_p \quad (5)$$

Where F_1 is magnetic force which acting on a single MDC and given by [21]:

$$\vec{F}_1 = 0.5 \times \nabla_{MNP} \times \mu_0 \frac{\chi_{MNP}}{1 + \chi_{MNP}/3} \times \nabla |H|^2 \quad (6)$$

∇_{MNP} is total volume of magnetic nanoparticles in single MDC and χ_{MNP} is the magnetic susceptibility of the magnetic nanoparticles sand set equal to 2 [22].

Number of MDCs is unit of volume, n_p , is obtained from:

$$n_p = \frac{C_{MDC}}{\nabla_{MDC}} = C \times \frac{C_0}{\nabla_{MDC}} \quad (7)$$

Where C_{MDC} , C_0 and C are volumetric concentration of MDCs in the blood, concentration of MDCs at inlet and dimensionless concentration (C_{MNP}/C_0), respectively.

By combining equations (5), (6) and (7), the volume force becomes:

$$\vec{F} = \frac{1}{2} \mu_0 \frac{\chi_{MNP}}{1 + \chi_{MNP}/3} \frac{\nabla_{MNP}}{\nabla_{MDC}} C_0 C \nabla |H|^2 \quad (8)$$

Inserting equation (8) into equations (3) and (4), the horizontal and vertical momentum equations become, respectively:

$$\rho \frac{\partial u}{\partial t} + \rho \left(u \frac{\partial u}{\partial x} + v \frac{\partial u}{\partial y} \right) = -\frac{\partial p}{\partial x} + \mu \left(\frac{\partial^2 u}{\partial x^2} + \frac{\partial^2 u}{\partial y^2} \right) + \left[\frac{1}{2} \mu_0 \frac{\chi_{MNP}}{1 + \chi_{MNP}/3} \frac{\nabla_{MNP}}{1 + \nabla_{MDC}} \frac{\partial}{\partial x} |H|^2 \right] C_0 C \quad (9)$$

$$\rho \frac{\partial v}{\partial t} + \rho \left(u \frac{\partial v}{\partial x} + v \frac{\partial v}{\partial y} \right) = -\frac{\partial p}{\partial y} + \mu \left(\frac{\partial^2 v}{\partial x^2} + \frac{\partial^2 v}{\partial y^2} \right) + \left[\frac{1}{2} \mu_0 \frac{\chi_{MNP}}{1 + \chi_{MNP}/3} \frac{\nabla_{MNP}}{1 + \nabla_{MDC}} \frac{\partial}{\partial y} |H|^2 \right] C_0 C \quad (10)$$

The concentration equation (mass transfer) inside the capillary is as follow [10]:

$$\frac{\partial C}{\partial t} = \nabla \cdot (D_{blood} \nabla C) - \nabla \cdot (C \vec{v}_{MDC}) \quad (11)$$

First term in right hand of equation (11) is diffusion due to concentration gradient where D_{blood} is MDCs diffusion coefficient in blood.

MDCs diffusion coefficient is given by (9):

$$D_{Blood} = D_B + D_S \quad (12)$$

Where D_B is Brownian diffusion coefficient and it is calculated from Einstein relation (9):

$$D_B = \frac{K_B T}{6\pi\mu_{blood}r_{MDC}} \quad (13)$$

D_S is scattering diffusion coefficient and it is equal to 3.5×10^{-12} [14].

Also second term is mass transfer due to convection where \vec{v}_{MDC} is MDCs velocity vector and calculated by:

$$\vec{v}_{MDC} = \vec{v} + \vec{v}_{relative} \quad (14)$$

$v_{relative}$ is the MDCs relative velocity with respect to the blood flow and it is given by [13]:

$$\vec{v}_{relative} = \frac{\vec{F}_1}{6\pi\mu_{blood}r_{MDC}} = \frac{\nabla_{MNP}}{12\pi\mu_{blood}r_{MDC}} \times \mu_0 \frac{\chi_{MNP}}{1 + \chi_{MNP}/3} \times \nabla |H|^2 \quad (15)$$

Inserting equations (14) and (15) into equation (11) gives:

$$\frac{\partial C}{\partial t} = -\nabla \cdot \left[-D_{Blood} \nabla C + C \vec{v} + C \frac{\nabla_{MNP}}{12\pi\mu_{blood}r_{MDC}} \mu_0 \frac{\chi_{MNP}}{1 + \chi_{MNP}/3} \nabla (|H|^2) \right] \quad (16)$$

Where the magnetic field intensity (H) is given by [21]:

$$H = \frac{B_0}{\mu_0} \frac{r_{mag}^2}{(x - x_{mag})^2 + (y - y_{mag})^2} \quad (17)$$

where B_0 is magnetic flux density of external magnet at its surface.

The last term in right hand of equation (16) is mass transfer due to magnetic force (influence of external magnet). As shown this term is function of $\left(\frac{\nabla_{MNP}}{r_{MDC}} \right)$. By inserting ∇_{MNP} from equation (1) the term $\left(\frac{\nabla_{MNP}}{r_{MDC}} \right)$ is as follow:

$$\frac{\nabla_{MNP}}{r_{MDC}} = \frac{0.7(\nabla_{MDC} - \nabla_{shell})}{r_{MDC}} = \frac{2.8\pi(r_{MDC} - 5e(-9))^3}{3r_{MDC}} \quad (18)$$

This means that this term becomes greater as MDCs radius (r_{MDC}) increases.

3.3. In the Endothelium Layer

One row of adjacent Endothelium cells consist capillary wall but there are thin slits between adjacent Endothelium cells. The width of these slits is only about 6 to 7nm [19, 20]. But the blood vessels in tumor tissue have defective architecture and pores cut-off size in these capillaries is so much greater. In this study the Endothelium layer intercellular gap is set equal to 500nm, which is the actual cut-off size for LST174T tumor [5, 23].

Capillary wall is modelled as a saturated porous media. Therefore, the concentration equation is [24]:

$$\frac{\partial C}{\partial t} = -\nabla \cdot [-D_{Endo} \nabla C + C \vec{V}_{MDC}] + \frac{G}{\varepsilon} - E(C) \quad (19)$$

G and E are generation and uptake terms, respectively. In this study no generation and no uptake is considered.

The MDCs diffusion coefficient in Endothelium layer (D_{Endo}) is given by [20, 24]:

$$D_{endo} = D_{\infty} \times \left(\frac{\varepsilon}{\lambda_g^2} \right) \times S \times J \quad (20)$$

Where D_{∞} is diffusion coefficient of particle in unbounded fluid and ε and λ_g are porosity and geometrical tortuosity of Endothelium layer. Also S and J are steric coefficient and hydrodynamic coefficient of MDCs in Endothelium layer, respectively.

MDCs diffusion coefficient in unbounded fluid, D_{∞} , is given by Brownian diffusion coefficient of particles in the plasma, because of the gaps between endothelial cells is filled with plasma, and is as follows:

$$D_{plasma} = \frac{k_B T}{6\pi\mu_{plasma} r_{MDC}} \quad (21)$$

Where μ_{plasma} is plasma viscosity and it is equal to 1.24 mPa.s [25, 26].

The porosity (ε) of Endothelium layer is obtained by:

$$\varepsilon = \frac{\text{Intercellular gap in Endotheium layer}}{\text{Average size of Endotheium cell}} \quad (22)$$

The geometrical tortuosity square (λ_g^2) of Endothelium layer is set equal to 2.

It is worth mentioning that hydrodynamic coefficient appears when channel radius is comparable to particle radius and causes the fluid drag force to increase. The hydrodynamic coefficient (J) and steric coefficient (S) of MDCs in Endothelium layer are given by [20, 27]:

$$J = (1 - 2.1044\alpha + 2.089\alpha^3 - 0.948\alpha^5) \quad (23)$$

$$S = (1 - \alpha)^2, \alpha = \frac{r_{MDC}}{r_{Pore}} \quad (24)$$

Also, it is assumed that the fluid is motionless in Endothelium layer and the tissue where the maximum

velocity is very small (0.016 $\mu\text{m/s}$ for 1cm radius tumor surrounded with normal tissue). This is documented by Jain and Baxter [28]. Therefore, the MDCs velocity is the same as relative velocity as follows:

$$\vec{V}_{MDC} = \varepsilon \left(\frac{1}{\lambda_g^2} \right) S \times J \frac{\vec{F}_1}{6\pi\mu r_{MDC}} = \varepsilon \left(\frac{1}{\lambda_g^2} \right) S \times J \frac{\nabla_{MNP}}{12\pi\mu r_{MDC}} \times \mu_0 \frac{\chi_{MNP}}{1 + \chi_{MNP}/3} \nabla(|H|^2) \quad (25)$$

3.4. In the Tumor Tissue

Like Endothelium layer, tumor tissue is modelled as porous media. The concentration equation in the tumor tissue is as follow:

$$\frac{\partial C}{\partial t} = -\nabla \cdot \left[-D_{Tissue} \nabla C + C \varepsilon \left(\frac{1}{\lambda_g^2} \right) \times S \times J \frac{\nabla_{MNP}}{12\pi\mu_{plasma} r_{MDC}} \mu_0 \frac{\chi_{MNP}}{1 + \chi_{MNP}/3} \nabla(|H|^2) \right] \quad (26)$$

The first term in right hand of equation (25) is diffusion due to concentration gradient and second term is penetration under the influence of magnet (magnetic term). This means that the MDCs penetrate due to two different mechanisms, diffusion and magnetic penetration. So the MDCs penetration is summation of two mechanisms effects.

Again, the MDCs diffusion coefficient in the tissue (D_{Tissue}) is obtained by:

$$D_{Tissue} = D_{\infty} \times \left(\frac{\varepsilon}{\lambda_g^2} \right) \times S \times J \quad (27)$$

MDCs diffusion coefficient in unbounded fluid, D_{∞} , is equal to D_{Plasma} because the interstitial fluid is same physical properties with plasma. The steric coefficient (S) and hydrodynamic coefficient (J) of MDCs in tissue are expressed by [29, 30]:

$$S = \exp(-0.84k^{1.09}), k = \left(1 + \frac{r_{MDC}}{r_{fiber}} \right)^2 \times \phi \quad (28)$$

$$J = e^{-\alpha \times \phi} \quad (29)$$

Where Φ is the fibers volume fraction. The value of α and v are listed in Table 1 [29].

Table 1: Amount of α and ν for Equ, 30

$r_{\text{fiber}} / r_{\text{MNP}}$	α	ν
0.1	3.483	0.354
0.2	3.248	0.434
0.29	2.871	0.477
0.4	3.146	0.532
0.6	2.526	0.518
0.75	2.500	0.600
1.0	1.900	0.600
2.0	2.114	0.1719

Collagen fibrils radius (r_{fibrils}) is set equal to 50nm. The value of r_{fibrils} is reported to be between 15 to 100nm [31, 32]. Also, the value of the fiber volume fraction (Φ) is set equal to 0.03 [33].

The geometrical tortuosity of tumor tissue can express as a function of porosity and given by [24]:

$$\lambda_g = \varepsilon^{-n} \tag{30}$$

Tissue porosity (ε) is varied between 0.06 and 0.6 for different tumors [34, 35, 36]. The value of n has an upper and lower limit and is determined by:

Upper limit: $n = 0.23 + 0.3\varepsilon + \varepsilon^2$

Lower limit: $n = 0.23 + \varepsilon^2$

In this study and average value of n is utilized.

4. BOUNDARY AND INITIAL CONDITION

4.1. Boundary Conditions

The boundary conditions according to Figure 3 are set as Table 2.

Table 2: Boundary Conditions

No.	Boundary	Conditions
1	Channel inlet	Steady velocity ($U_{in}=0.2 \text{ mm/s}$)[37] Steady MDCs inlet concentration ($C_0=10^{-4}$)
4	Channel upper wall	No slip condition ($u, v=0$) MNCs can go through the wall
3	Channel lower wall	No slip condition ($u, v=0$) MNCs can't go through the wall
2	Channel outlet	Neumann boundary condition for both momentum and concentration equations
5	Tissue upper wall	MDCs cannot go through the wall
6, 7	Tissue right and left wall	MDCs cannot go through the wall

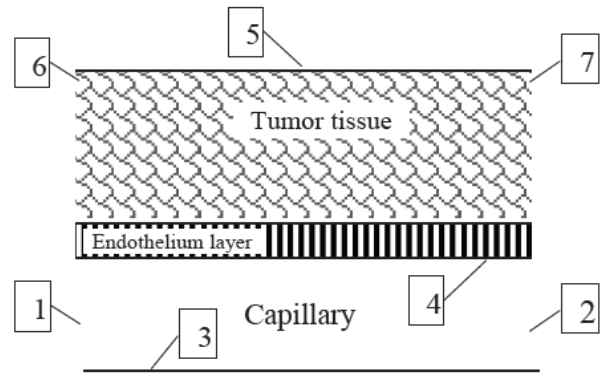


Figure 3: Schematic model and numbering of boundary conditions.

4.2. Initial Condition

Dimensionless MDCs concentration (C) inside the vessel is equal to 1 and no concentration is assumed in the capillary wall (Endothelium layer) and in the tumor tissue ($C=0$).

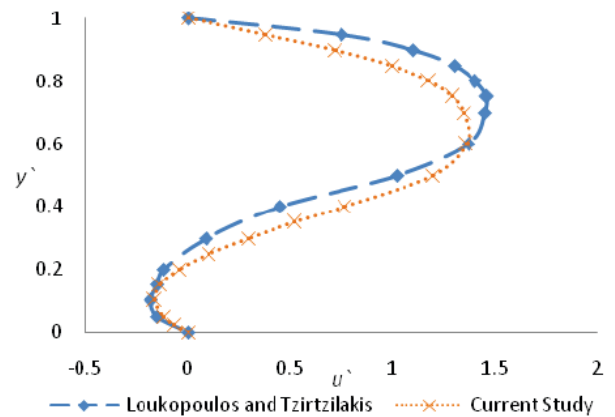


Figure 4: Comparison of Dimensionless Horizontal Velocity Profile in the Center of Vortex ($x'=3.5$).

4.3. Verification

For verification purpose, the result of the current study is compared with the numerical simulation documented by Loukopoulos and Tzirtzilak is [38].

Figure 4 depicts the highest critical point non-dimensional velocity profile (at the center of the vortex). As shown the results agrees well with that of the Loukopoulos and Tzirtzilak is results. The slight difference between the two results is due to the finite

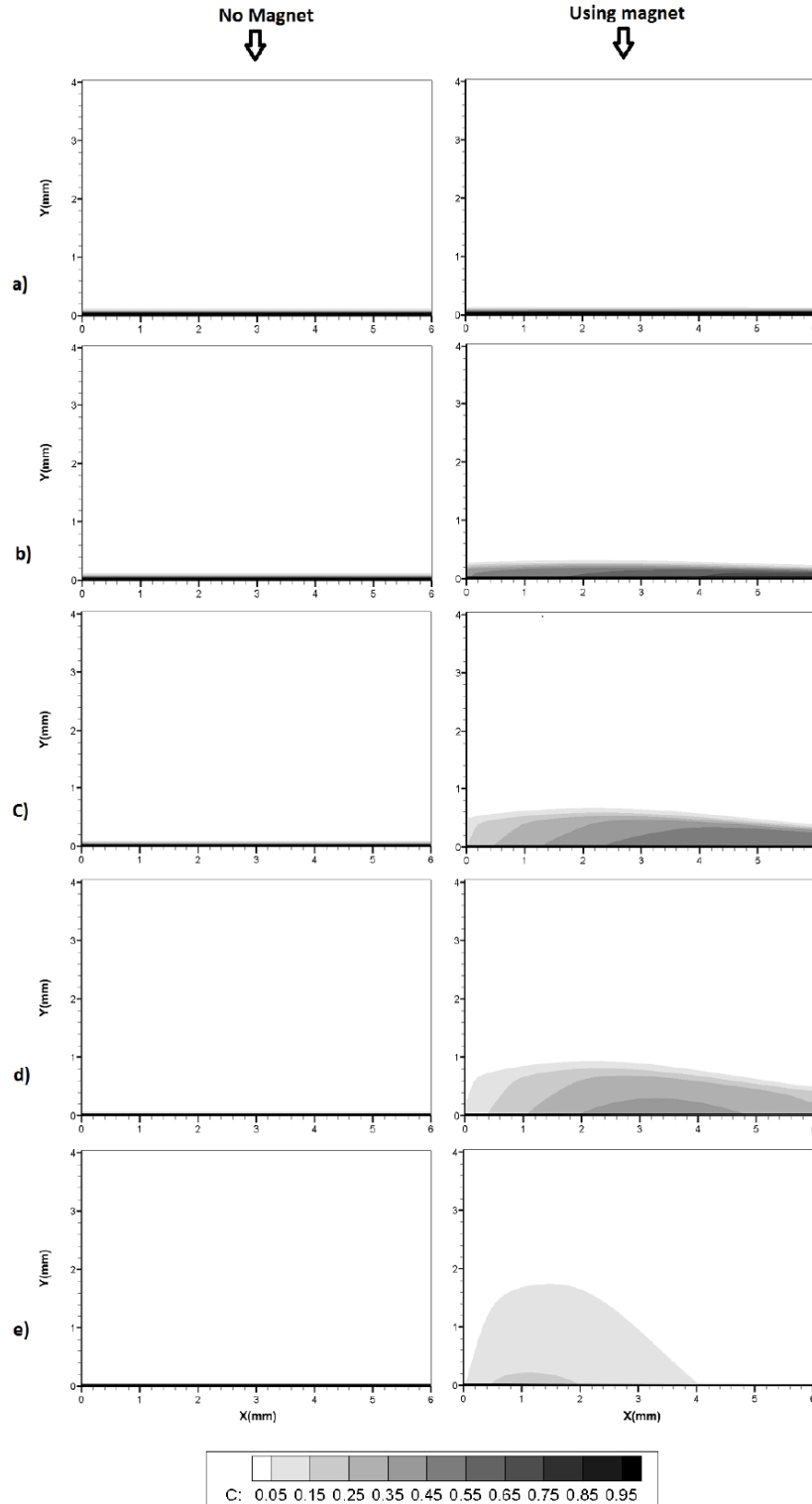


Figure 5: Dimensionless concentration distribution of MDCs in the tumor tissue at 1 hour time in absence and presence of external magnet. (a): 50nm, (b): 100nm, (c): 166nm, (d): 250nm, (e): 345nm MDCs (porosity=0.3, z=3mm).

volume method (FVM) used in the current study compared with finite difference method (FDM) used by Loukopoulos and Tzirtzilak is.

5. RESULTS AND DISCUSSION

An in house code based on finite volume is developed and utilized to solve the coupled governing nonlinear differential equations, mass, momentum and concentration. The code is based on the SIMPLE algorithm and written in FORTRAN. The code runs 1 hour per case and results are evaluated.

5.1. MDCs Concentration Distribution

Figure 5 shows the distribution of dimensionless MDCs concentration in the tumor tissue at 1hour time without and with applying external magnet. MDCs diameters are 50nm, 100nm, 166nm, 250nm and 345nm and magnetic flux density of external magnet set to 2 tesla.

As shown, for MDCs greater than 50nm, the penetration increases exponentially as the external magnet is applied. But the effect of the external magnet on the penetration of 50nm MDCs is minimal. This is because $\left(\frac{\nabla MNP}{r MDC}\right)$ (is small while MDCs are small (see equation 17) and therefore the magnetic penetration term is not significant and so external magnet dose not excessively affects the MDCs penetration.

5.2. Variation with Time

Figures 6 and 7 represent the time variation of average dimension less MDCs concentration (C_{ave}) without and with external magnet, respectively. The average dimensionless MDCs concentration parameter in the tissue (C_{ave}) is [29]:

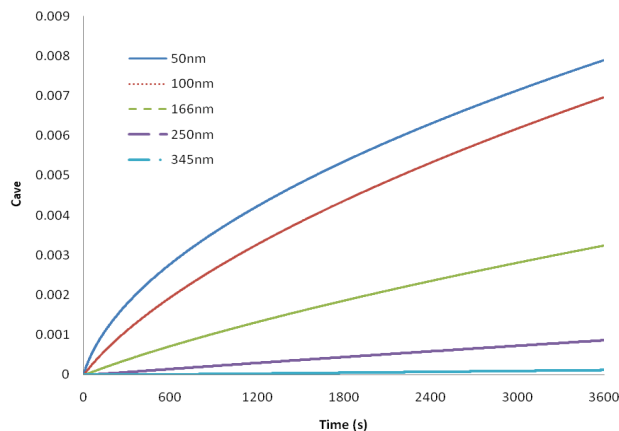


Figure 6: Time variation of average dimensionless MDCs concentration (C_{ave}) in absence of the external magnet. (Porosity=0.3, z=3mm).

$$C_{ave} = \frac{\sum C_i A_i}{\sum A_i} \quad (31)$$

where C_i is the MNPs dimensionless concentration, A_i is the area of i 'th computational cell and are summed over the whole tissue.

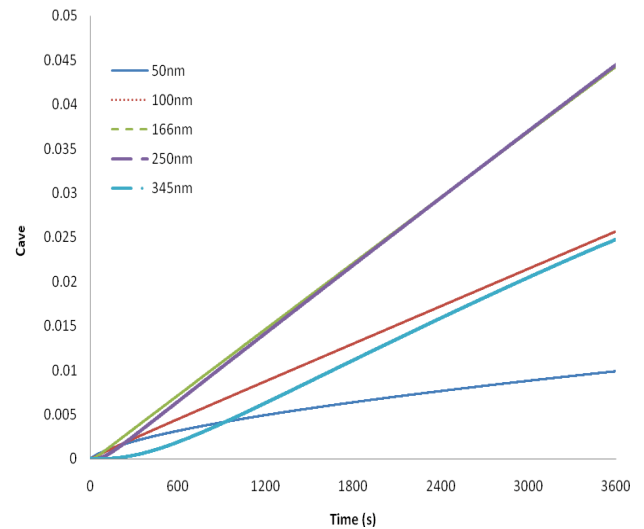


Figure 7: Time variation of average dimensionless MDCs concentration (C_{ave}) in presence of the external magnet. (Porosity=0.3, z=3mm).

As shown, in the absence of external magnet, the rate of C_{ave} decreases as time passes. This is because the gradient of MDCs concentration which causes the diffusion decreases as time passes. However, the presence of external magnet causes the average dimensionless MDCs concentration to increase constantly. This is because the magnetic term of MDCs penetration does not vary with time. Also, C_{ave} has been multiplied when external magnet applied.

CONCLUSION

The purpose of current study is to deliver the magnetic drug carries to the cancerous tumor tissue and enhance the penetration of them. In this study, the effect of external magnet on the MDCs concentration in the tumor tissue is numerically investigated. In order to solve the coupled governing equations, mass, momentum and concentration, an in house finite volume based code is developed and utilized. The effect of physical parameters on the MDCs concentration is investigated. The results show that in the absence of external magnet, even though the small MDCs penetrate deeper into the tumor and depict higher concentration but their penetration into the tumor in general is minimal and is limited to the surface of the tumor, which verifies the observations

documented by literatures. In the presence of external magnet the greater MDCs penetrate deeper into the tumor.

NOMENCLATURE

B_0	Magnetic flux density of external magnet at its surface.
C_0	MDCs concentration at inlet.
C	MDCs dimensionless concentration.
D	MDCs diffusion coefficient.
D_∞	Diffusion coefficient of particle in unbounded fluid.
D_{blood}	MDCs diffusion coefficient in the blood.
D_B	Brownian diffusion coefficient of MDCs.
D_S	Scattering diffusion coefficient of MDCs.
D_{Endo}	MDCs diffusion coefficient in the Endothelium layer.
D_{Tissue}	MDCs diffusion coefficient in the Tumor tissue.
E	Uptake term.
F_1	Magnetic force acting upon a single MDC.
F_x	Horizontal magnetic body force.
F_y	Vertical magnetic body force.
G	Generation term.
H	Magnetic field intensity.
J	Hydrodynamic coefficient.
P	Pressure.
Re	Reynolds number.
r_{mag}	External magnet radius.
S	Steric coefficient.
U_{in}	Inlet blood velocity.
u	Horizontal blood velocity.
v	Vertical blood velocity.
\vec{V}	Blood velocity vector.
\vec{V}_{MDC}	MDCs velocity vector.
$\vec{V}_{\text{relative}}$	Relative velocity of MDCs to blood.
x_{mag}	Horizontal position of external magnet.
y_{mag}	Vertical position of external magnet.

z	Distance between external magnet and tumor.
ρ	Blood density.
ϵ	Porosity.
μ	Blood viscosity.
μ_{plasma}	Plasma viscosity.
μ_0	Magnetic permeability of vacuum.
λ_g	Geometrical tortuosity.
χ	Magnetic susceptibility of the MNPs.
τ_p	Particle response time.
∇_{MNP}	Total volume of MNPs in single MDC.
∇_{MDC}	Volume of a single MDC.

REFERENCES

- [1] Pankhurst QA, Connolly J, Jones SK and Dobson J. Applications of magnetic nanoparticles in biomedicine. *Journal Of Physics D Applied Physics* 2003; 36: 167-181. <https://doi.org/10.1088/0022-3727/36/13/201>
- [2] Sarin H. Physiologic upper limits of pore size of different blood capillary types and another perspective on the dual pore theory of microvascular permeability. *Journal of Angiogenesis Research* 2010; 2. <https://doi.org/10.1186/2040-2384-2-14>
- [3] Okuhata Y. Delivery of diagnostic agents for magnetic resonance imaging. *Advanced Drug Delivery Reviews* 1999; 37: 121-137. [https://doi.org/10.1016/S0169-409X\(98\)00103-3](https://doi.org/10.1016/S0169-409X(98)00103-3)
- [4] Dreher MR, Liu W, Michelich CR, Dewhirst MW, Yuan F, et al. Tumor Vascular Permeability, Accumulation, and Penetration of Macromolecular Drug Carriers. *Journal of the National Cancer Institute* 2006; 98(5): 335-344. <https://doi.org/10.1093/jnci/djj070>
- [5] Yuan F, Dellian M, Fukumura D, Leunig M, Berk DA, et al. Vascular Permeability in a Human Tumor Xenograft: Molecular Size Dependence and Cutoff Size. *Cancer Research*. 1995; 55: 3752-3756.
- [6] Shaw and Murthy. Magnetic targeting in the impermeable microvessel with two-phase fluid model—Non-Newtonian characteristics of blood. *Microvascular Research* 2010; 80: 209-220. <https://doi.org/10.1016/j.mvr.2010.05.002>
- [7] Khashan SA and Furlani EP. Effects of particle–fluid coupling on particle transport and capture in a magnetophoretic microsystem. *Microfluid Nanofluid* 2012; 12: 565-580. <https://doi.org/10.1007/s10404-011-0898-y>
- [8] Sharma S, Singh U and Katiyar VK. Modeling and in vitro study on capture efficiency of magnetic nanoparticles transported in an implant assisted cylindrical tube under magnetic field. *Microfluid Nanofluid* 2015; 19: 1061-1070. <https://doi.org/10.1007/s10404-015-1647-4>
- [9] Grief A and Richardson G. Mathematical modelling of magnetically targeted drug delivery. *Journal of Magnetism and Magnetic Materials* 2005; 293: 455-463. <https://doi.org/10.1016/j.jmmm.2005.02.040>
- [10] Habibi MR and Ghasemi M. Numerical study of magnetic nanoparticles concentration in biofluid (blood) under influence of high gradient magnetic field. *Journal of Magnetism and Magnetic Materials* 2011; 323: 32-38. <https://doi.org/10.1016/j.jmmm.2010.08.023>

- [11] Li XL, Yao KL and Liu ZL. CFD study on the magnetic fluid delivering in the vessel in high-gradient magnetic field. *Journal of Magnetism and Magnetic Materials* 2008; 320: 1753-1758.
<https://doi.org/10.1016/j.jmmm.2008.01.041>
- [12] Cao Q, Han X and Li L. Numerical analysis of magnetic nanoparticle transport in microfluidic systems under influence of permanent magnets. *Journal of Physics D Applied Physics* 2012; 45(46).
<https://doi.org/10.1088/0022-3727/45/46/465001>
- [13] Habibi MR, Ghassemi M and Hamed MH. Analysis of high gradient magnetic field effects on distribution of nanoparticles injected into pulsatile blood stream. *Journal of Magnetism and Magnetic Materials* 2012; 324: 1473-1482.
<https://doi.org/10.1016/j.jmmm.2011.11.022>
- [14] Nacev A, Beni C, Bruno O and Shapiro B. The behaviors of ferromagnetic nano-particles in and around blood vessels under applied magnetic fields. *Journal of Magnetism and Magnetic Materials* 2011; 323: 651-668.
<https://doi.org/10.1016/j.jmmm.2010.09.008>
- [15] Klinbun W, Vafai K and Rattanadecho P. Electromagnetic field effects on transport through porous media. *International Journal of Heat and Mass Transfer* 2012; 55: 325-335.
<https://doi.org/10.1016/j.ijheatmasstransfer.2011.09.022>
- [16] Khanafer K, Vafai K and Kangarlou A. Computational modeling of cerebral diffusion-application to stroke imaging. *Magnetic Resonance Imaging* 2003; 21: 651-661.
[https://doi.org/10.1016/S0730-725X\(03\)00091-2](https://doi.org/10.1016/S0730-725X(03)00091-2)
- [17] Keangin P and Vafai KPR. Electromagnetic field effects on biological materials. *International Journal of Heat and Mass Transfer* 2013; 65: 389-399.
<https://doi.org/10.1016/j.ijheatmasstransfer.2013.06.039>
- [18] Hashizume H, Baluk P, Morikawa S, McLean JW, Thurston G, et al. Openings between Defective Endothelial Cells Explain Tumor Vessel Leakiness. *American Journal of Pathology* 2000; 156: 1363-1380.
[https://doi.org/10.1016/S0002-9440\(10\)65006-7](https://doi.org/10.1016/S0002-9440(10)65006-7)
- [19] Waite L and Fine J. *Applied biofluid mechanics* Chicago: McGraw-Hill 2007.
- [20] Fournier RL. *Basic Transport Phenomena in Biomedical Engineering* New York: CRC Press 2011.
- [21] Berthier and Silberzan. *Microfluidics for biotechnology*. 1st ed. Boston: Artech House, Inc 2006.
- [22] Lunnoo T and Puangmali T. Capture Efficiency of Biocompatible Magnetic Nanoparticles in Arterial Flow: A Computer Simulation for Magnetic Drug Targeting. *Nanoscale Research Letters* 2015; 10: 426.
<https://doi.org/10.1186/s11671-015-1127-5>
- [23] Hobbs. Regulation of transport pathways in tumor vessels: role of tumor type and microenvironment. *Proceedings of the National Academy of Sciences of the United States of America* 1998; 95: 4607-4612.
<https://doi.org/10.1073/pnas.95.8.4607>
- [24] Khanafer k and Vafai k. The Role of Porous Media in Biomedical Engineering as Related to Magnetic Resonance Imaging and Drug Delivery. *Heat Mass Transfer* 2006; 42: 939-953.
<https://doi.org/10.1007/s00231-006-0142-6>
- [25] Windberger , Bartholovitsch, Plasenzotti and Korak and Heinze. Whole blood viscosity, plasma viscosity and erythrocyte aggregation in nine mammalian species reference values and comparison of data. *Experimental Physiology Translation and Integration* 2003; 88(3): 431-440.
<https://doi.org/10.1113/eph8802496>
- [26] Késmárky G, Kenyeres , Rábai M and Tóth K. Plasma viscosity: a forgotten variable. *Clinical Hematology* 2008; 39: 243-246.
- [27] Ai L and Vafai K. A coupling model for macromolecule transport in a stenosed arterial wall. *International Journal of Heat and Mass Transfer* 2006; 49: 1568-1591.
<https://doi.org/10.1016/j.ijheatmasstransfer.2005.10.041>
- [28] Jain RK and Baxter LT. Mechanisms of Heterogeneous Distribution of Monoclonal Antibodies and Other Macromolecules in Tumors: Significance of Elevated Interstitial Pressure. *Cancer Research* 1988; 48: 7022-7032.
- [29] Saltzman WM. *Drug Delivery Engineering Principles for Drug Therapy*: Oxford University Press 2001.
- [30] Swartz MA and Fleury ME. Interstitial flow and its effects in soft tissues. *Annual Review of Biomedical Engineering* 2007; 9: 229-256.
<https://doi.org/10.1146/annurev.bioeng.9.060906.151850>
- [31] Wenger MPE, Bozec L, Horton MA and Mesquida P. Mechanical Properties of Collagen Fibrils. *Biophysical Journal* 2007; 93: 1255-1263.
<https://doi.org/10.1529/biophysj.106.103192>
- [32] Kim DH, Lipke EA, Kim P, Cheong R, Thompson S, et al. Nanoscale cues regulate the structure and function of macroscopic cardiac tissue constructs. *Applied Biological Sciences* 2010; 107(2): 565-570.
<https://doi.org/10.1073/pnas.0906504107>
- [33] Ramanujan S, Pluen A, McKee TD, Brown EB, Boucher Y and Jain RK. Diffusion and Convection in Collagen Gels: Implications for Transport in the Tumor Interstitium. *Biophysical Journal* 2002; 83: 1650-1660.
[https://doi.org/10.1016/S0006-3495\(02\)73933-7](https://doi.org/10.1016/S0006-3495(02)73933-7)
- [34] Graff BA, Bjørnæs I and Rofstad EK. Macromolecule uptake in human melanoma xenografts: relationships to blood supply, vascular density, microvessel permeability and extracellular volume fraction. *European Journal of Cancer* 2000; 36: 1433-1440.
[https://doi.org/10.1016/S0959-8049\(00\)00120-9](https://doi.org/10.1016/S0959-8049(00)00120-9)
- [35] Bhujwala Z, McCoy C, Glickson J, Gilfies R and Stubbs M. Estimations of intra- and extracellular volume and pH by 31p magnetic resonance spectroscopy: effect of therapy on RIFm1 tumours. *BshJournal of Cancer* 1998; 78(5): 606-611.
<https://doi.org/10.1038/bjc.1998.548>
- [36] Jain RK. Transport of Molecules in the Tumor Interstitium: A Review. *Cancer Research* 1987; 47: 3039-3051.
- [37] Jain RK and Stylianopoulos T. Delivering nanomedicine to solid tumors. *Nature Reviews Clinical Oncology* 2010; 7: 653-664.
<https://doi.org/10.1038/nrclinonc.2010.139>
- [38] Loukopoulos and Tzirtzilakis. Biomagnetic channel flow in spatially varying magnetic field. *International Journal of Engineering Science* 2004; 42: 571-590.
<https://doi.org/10.1016/j.ijengsci.2003.07.007>